

# Fabrication of Surface Plasmon Resonators by Nanoskiving Single-Crystalline Gold Microplates

Benjamin J. Wiley,<sup>†</sup> Darren J. Lipomi,<sup>†</sup> Jiming Bao,<sup>‡</sup> Federico Capasso,<sup>‡</sup> and George M. Whitesides<sup>\*†</sup>

*Department of Chemistry and Chemical Biology, Harvard School of Engineering and Applied Sciences, Harvard University, 12 Oxford Street, Cambridge, Massachusetts 02138*

*Received July 25, 2008; Revised Manuscript Received August 4, 2008*

## ABSTRACT

This paper demonstrates the sectioning of chemically synthesized, single-crystalline microplates of gold with an ultramicrotome (nanoskiving) to produce single-crystalline nanowires; these nanowires act as low-loss surface plasmon resonators. This method produces collinearly aligned nanostructures with small, regular changes in dimension with each consecutive cross-section: a single microplate thus can produce a number of “quasi-copies” (delicately modulated variations) of a nanowire. The diamond knife cuts cleanly through microplates 35  $\mu\text{m}$  in diameter and 100 nm thick without bending the resulting nanowire and cuts through the sharp edges of a crystal without deformation to generate nanoscale tips. This paper compares the influence of sharp tips and blunt tips on the resonator modes in these nanowires.

**Introduction.** This paper describes the fabrication of single-crystalline gold nanowires by sectioning chemically synthesized single-crystalline microplates with an ultramicrotome (nanoskiving) and demonstrates that these wires can act as surface plasmon resonators. They are the first gold nanowires to exhibit this property (silver nanowires have been shown by Ditlbacher et. al<sup>1</sup> to be resonators); the single-crystalline gold nanowires fabricated here have much lower radiative loss than polycrystalline nanowires. Nanowires produced by nanoskiving are collinearly aligned and have small, regular variations in size and interwire distances from section to section; they are thus exceptionally useful as subjects for spectroscopic studies involving comparisons of structures differing in nanometer scale dimensions. By combining chemical synthesis of single-crystalline metallic plates with nanoskiving, we demonstrate a new strategy for preparing single-crystalline nanostructures and for studying the coupling of light between these nanostructures. These studies suggest new types of nanophotonic devices based on low-loss single-crystalline plasmonic waveguides.

**Background.** The miniaturization of optical waveguides, lenses, and resonators based on dielectric materials is limited by diffraction to about half the wavelength of light in the material. One way to circumvent the limits of diffraction is to couple light into a surface plasmon mode confined to a

metal-dielectric interface.<sup>2</sup> Strips of evaporated metal with subwavelength (nanoscale) diameters are capable of guiding light at the nanoscale, but these waveguides suffer from high loss (the propagation length of light in these structures is around 2.5  $\mu\text{m}$ ).<sup>3,4</sup> In chemically synthesized silver nanowires, this propagation length increases to 10  $\mu\text{m}$  because of their smooth surfaces.<sup>1</sup> The low loss of these silver nanowires gives them the ability to act as surface plasmon resonators, a characteristic that polycrystalline metal nanowires do not possess.<sup>1</sup> A disadvantage of using silver nanowires for optical applications is that they oxidize after several days under ambient conditions.<sup>5</sup> The ability to prepare and use single-crystalline gold nanowires would circumvent this problem, but there have been no studies of the waveguiding and resonator properties of such structures.

**Experimental Design.** In nanoskiving, an ultramicrotome cuts a slab of a polymer block containing an embedded, vertically thin first structure and forms a laterally thin second structure.<sup>6</sup> We have used nanoskiving to fabricate wires, rings, and periodic arrays of shapes that possessed a range of optical properties.<sup>7–10</sup> All of these previous applications have started with physically deposited, polycrystalline thin films, which in turn generated polycrystalline nanostructures. To increase the quality of the nanostructures made by nanoskiving, we have developed a tandem technique comprising two steps: (i) chemical synthesis of single-crystalline gold microplates, and (ii) sectioning of these plates perpendicular to their plane to yield single-crystalline gold nanowires (Figure 1 summarizes the procedure). Remarkably, the

\* To whom correspondence should be addressed. E-mail: gwhitesides@gmwwgroup.harvard.edu.

<sup>†</sup> Department of Chemistry and Chemical Biology, Harvard University.

<sup>‡</sup> Harvard School of Engineering and Applied Sciences, Harvard University.

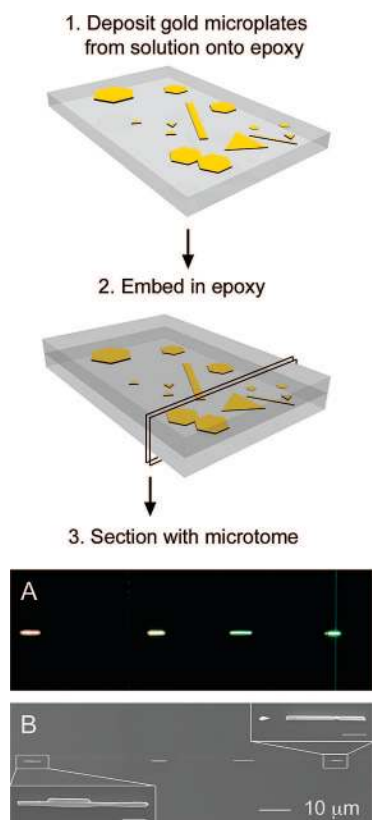


**Figure 1.** Schematic drawing of the procedure used to fabricate single-crystalline nanowires. We deposited microplates from solution onto a thin slab of epoxy and embedded a piece of this slab so that the plates were entirely surrounded by epoxy. (A) Optical image of a 100-nm-thick section in which aligned, single-crystalline gold nanowires are embedded. (B) SEM image of the same region shown in the optical image.

sectioning leaves the crystalline order of the gold plates largely or completely intact.

The gold microplates grew in a solution containing ethylene glycol (EG),  $\text{HAuCl}_4$ , and polyvinylpyrrolidone (PVP).<sup>11</sup> We prepared a flat piece of epoxy (Epo-fix, Electron Microscopy Sciences) by puddle-casting the prepolymer against the flat surface of a Si/SiO<sub>2</sub> wafer. After curing, we detached the epoxy from the Si/SiO<sub>2</sub> and deposited a suspension of the microplates on the flat side of the epoxy substrate. We adjusted the concentration of plates empirically to give the desired coverage of the surface (approximately 25%). After drying and rinsing to remove PVP, we embedded this substrate (epoxy and microplates) in additional epoxy and sectioned it with an ultramicrotome equipped with a diamond knife (Diatome Ultra 35).<sup>8</sup> It was straightforward to transfer the resulting thin (50 nm) epoxy slabs ( $\leq 1 \text{ mm}^2$ ) containing nanowires onto almost any substrate; we used glass coverslips or Si/SiO<sub>2</sub> wafers. Exposure to an oxygen plasma removed the embedding epoxy and left free-standing nanowires. Chemical synthesis determined the width (90–200 nm) and the length ( $\leq 40 \mu\text{m}$ ) of the nanowires, while the ultramicrotome determined the height (tunable from 10 to 1000 nm).

**Results and Discussion.** Sectioning the embedded microplates gave 50-nm-high gold nanowires embedded in epoxy; these wires were easily resolved using dark-field

optical microscopy (Figure 1A). The random spacing and dimensions (lengths, widths) of nanowires, together with the fact that there were few wires along the slab, greatly simplified correlating scanning electron microscope (SEM) images with optical images of the same nanowires (Figure 1B). Note that the nanowire on the far left of Figure 1A scatters more red light, and that on the far right scatters more green light. The magnified views of nanowires in the insets of Figure 1B (scale bar =  $1 \mu\text{m}$ ) show that two nanowires stuck together scatter red light (bottom left), and a nanowire aligned with a nanoparticle scatters green light (upper right). A defect in the diamond knife created a score mark (green line) across the epoxy slab and through the nanowire on the far right.

**Morphology of Microplates and Nanowires.** The single-crystalline gold microplates obtained from the reaction and deposition step consisted of hexagonal, triangular, and ribbon-like structures with diameters ranging from 1 to  $40 \mu\text{m}$  (Figure 2A). The thickness of these microstructures was usually between 90 and 200 nm. The inset in Figure 2A is a magnified image of a representative microplate: it is  $25 \mu\text{m}$  in diameter and ca. 100 nm thick. This thickness corresponds to the width of the gold nanowire in Figure 2B; this wire was obtained by sectioning a microplate  $35 \mu\text{m}$  in diameter. Although this microplate has a ratio of length to thickness of 350, the diamond knife cuts cleanly through it without bending the resulting nanowire. The inset gives a magnified view of a short rod along the side of the larger wire; the thin white line running parallel to the long wire is the edge of the epoxy that has delaminated from the wire. This arrangement of paired rod and wire reflects the sectioning of a small plate on top of a larger plate.

Treating the samples with oxygen plasma removed the epoxy matrix and generated freestanding, gold nanowires. This action made it possible to examine the sides of the nanowires. The SEM image of a gold nanowire in Figure 2C shows that the facet cut by the diamond knife (top of the wire) appears to be as smooth as the sides of the original crystal. The sharp tip at the end of the rod (inset) demonstrates that the diamond knife can cut through sharp edges of microplates with minimal disturbance and generate nanoscale tips free of bends or deformation. The lack of contrast across a nanowire when viewed under the transmission electron microscope (TEM) suggests it retained the single-crystalline structure of the original microplate (Figure 2D). The inset is a magnified view of the edge of the plate, which reveals defect free (111) lattice fringes and a nearly atomically smooth sidewall.

Figure 3 shows SEM images of gold nanostructures in five (of six; one slice is missing between B and C) consecutive sections to illustrate a unique aspect of nanoslicing. The position and dimensions of the large wire on the left remained roughly the same because the microtome cut thin ( $\leq 50 \text{ nm}$ ) sections of a crystal  $8 \mu\text{m}$  in diameter. Successive slabs produced controlled, regular, small variations in size for the smaller structure on the right, which are probably sections from the edge of a smaller, triangular microplate. The magnified images of the smaller structure (Figure 3F,G) again

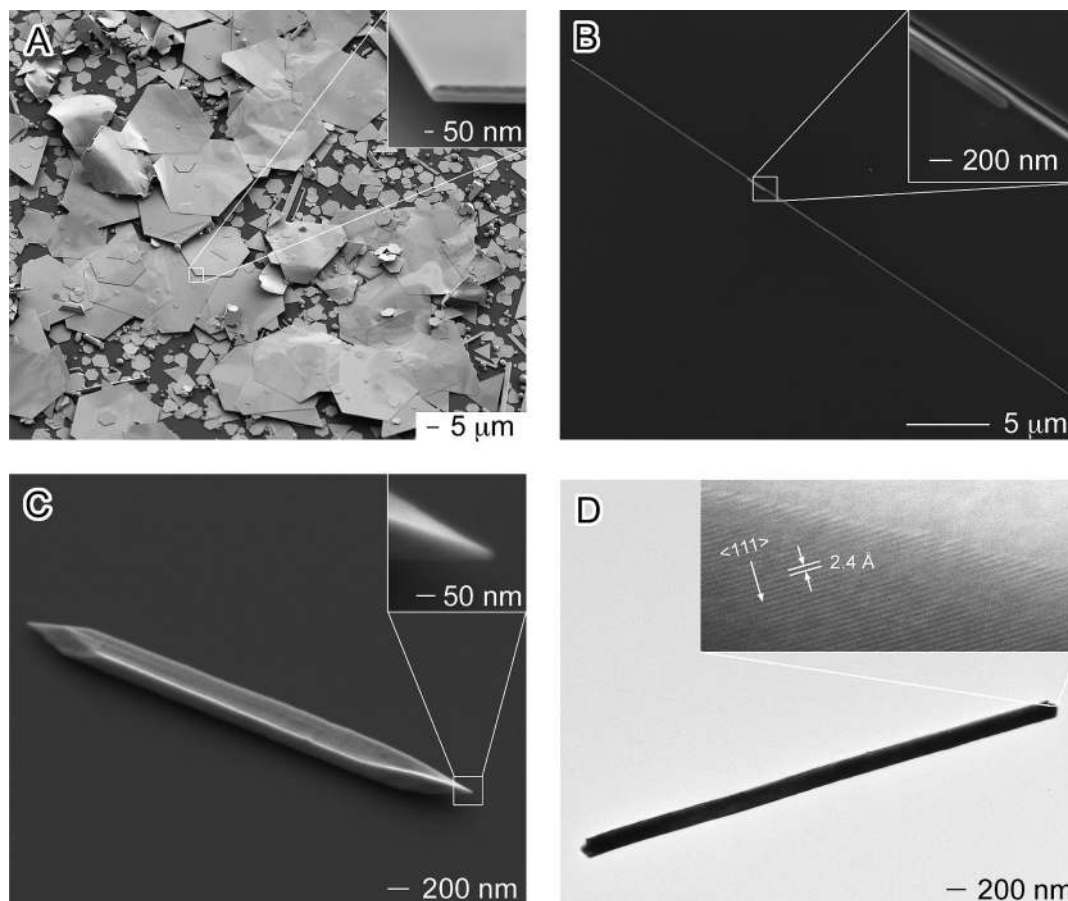


**Figure 2.** (A) SEM image of a substrate with a dense coverage of gold microplates to illustrate the variety of shapes and sizes produced by the synthesis. A slightly less dense, submonolayer coverage of microplates is best for producing isolated nanowires. The inset shows the 100-nm-thick edge of a 25- $\mu\text{m}$ -wide microplate. (B) SEM of a gold nanowire 35  $\mu\text{m}$  long and 100 nm wide obtained by nanoskiving a microplate. (C) SEM image of a gold nanowire with pointed tips obtained by nanoskiving. We removed the epoxy by etching with oxygen plasma to reveal the smooth sidewalls of the nanorod. (D) TEM image of a gold nanowire. The fringes indicate that the nanowire retained the crystal structure of the original synthesized microplate.

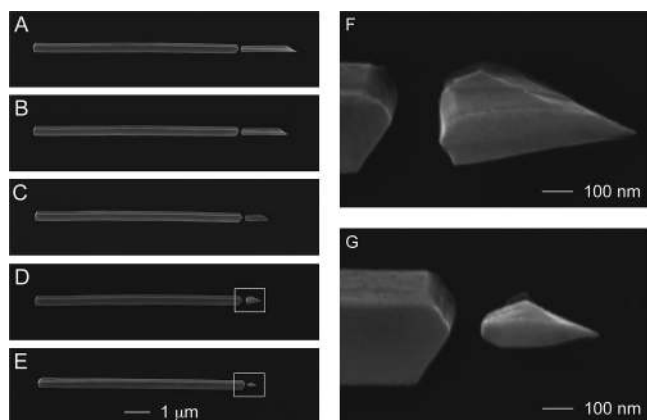


**Figure 3.** (A–E) SEM images of successive slabs illustrate nanoskiving can approximately reproduce the size and position of a nanowire as well as produce small, regular variations in size from section to section. (F,G) Magnified views of two nanoparticles with sharp tips collinearly aligned with the nanowire.

show that nanoskiving of crystals can result in remarkably sharp nanoscale tips. Crystals with sharp tips (similar to Figure 2C or Figure 3F,G) could be found in greater than 90% of the slabs; roughly 20% of nanowires had sharp tips.

The spacing between the two structures varied by less than 100 nm for all the slices.

Because each slab in nanoskiving can be registered with the following and preceding slabs, this method allows the generation of a sequence of structures with highly regular slab-to-slab changes. Precise, end-to-end alignment of nanowires deposited from solution is very difficult, but nanowires produced from nanoskiving are aligned collinearly every time with any other nanocrystals codeposited on the flat epoxy. This method is, thus, ideal for generating aligned arrays of nanostructures with spacings that are smoothly modulated (at least over several slabs), if presently random. These structures are very attractive for research in plasmonics because they allow detailed examination of dimensions and spacings at the scale of 10 nm.

**Characterization of the Plasmonic Properties of the Nanowire.** The smooth sidewalls of the gold nanowires suggested they might act as plasmon resonators. We tested this hypothesis by illuminating nanowires with unpolarized, focused white light from a tungsten lamp through a glass prism under total internal reflection (Figure 4A). Epoxy slabs containing nanowires were placed on a glass coverslip, etched

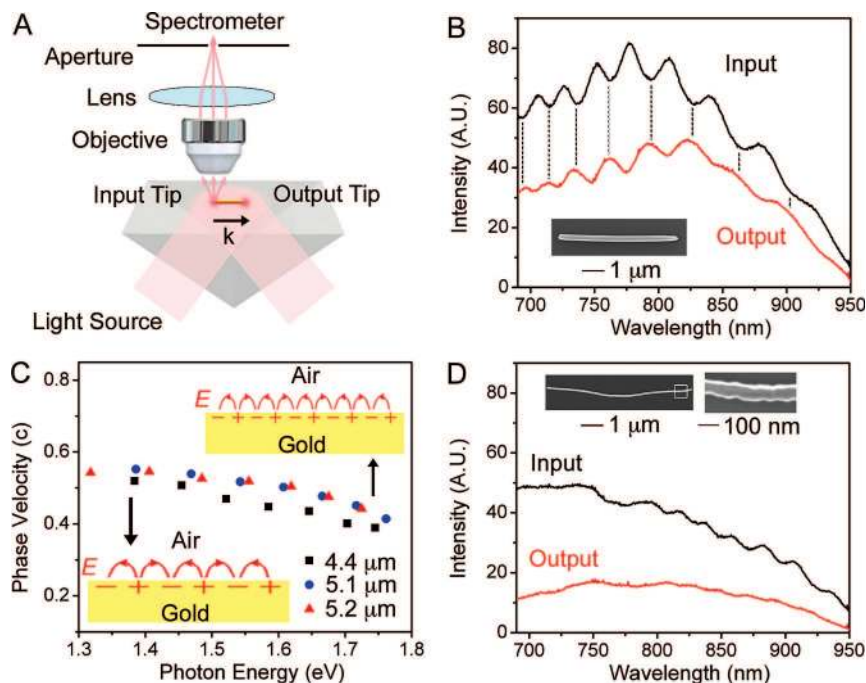


**Figure 4.** (A) Illustration showing the coupling of light into gold nanowires with illumination by total internal reflection on a prism. The input and output tip faced toward and away from the light source, respectively. Light radiated only from the ends of the nanowire, and this light was directed one end at a time into a spectrometer. (B) Spectra of the light reflected from the input and transmitted through the output ends of the single-crystalline nanowire shown in the inset SEM image. The wavelength-dependent periodic modulation of light and the correspondence between the reflection minima and the transmission maxima indicate the nanowire acted as a surface plasmon resonator. (C) The relative phase velocity of the surface plasmons decreased as the frequency increased on gold nanowires with three different lengths. Insets show the difference in the wavelength of the surface plasmon (induced surface charge) at the lowest and highest frequency. (D) Spectra of the light emitted from the ends of a polycrystalline wire indicate the surface plasmon was damped relative to the single-crystalline nanowire. The damping was due to the greater surface roughness of the polycrystalline wire, shown in the SEM image in the inset.

with oxygen plasma to remove the epoxy, and optically coupled to the prism with index-matching silicone oil.

We oriented the nanowires to be parallel to the wave vector of the evanescent wave generated at the interface between air and the glass coverslip. Although the nanowires are illuminated uniformly with a spot ca. 1 mm in diameter, light can couple into a propagating plasmon only at the end of the nanowire pointing toward the illumination source (defined as the input end in Figure 4A).<sup>1</sup> Plasmons can scatter as light at the ends of the wire; light does not radiate from the middle of the nanowire because the wave vector of a surface plasmon is greater than that of light in air. Significant roughness with a Fourier component corresponding to the momentum mismatch between the surface plasmon and light in air is required to couple light out from the middle of the wire. We collected the light radiated from the ends of the nanowire with a microscope objective (Mitutoyo SL50, numerical aperture (NA) = 0.55). The collected light passed through a polarizer oriented parallel to the long axis of the nanowire, a 665 nm long-pass colored glass filter, and focused on the plane of the entrance slit of a single-grating monograph (Jobin Yvon Horiba Triax 550); this apparatus allowed us to observe the nanowires on a monitor and measure their spectrum. We closed the entrance slits until only the light emitting from one end of the nanowire could be observed on the monitor before taking spectra.

Surface plasmons can reflect off the ends of the nanowire multiple times before radiating from an end as light; this geometry is similar to that of a Fabry–Perot etalon, i.e., a dielectric slab in which light undergoes multiple reflections. The only modes within a lossless resonator that can perpetuate are those that reproduce themselves after a single round trip; all other waves undergo destructive interference. The light transmitted through a surface plasmon resonator (and that reflected by it) consists of peaks separated by a wavelength difference,  $\Delta\lambda$ , given by eq 1, where  $\lambda$  is the free space

$$\Delta\lambda = \frac{\lambda^2 v_p}{2dc} \quad (1)$$

wavelength,  $v_p$  is the phase velocity of the plasmons,  $d$  is the length of the nanowire, and  $c$  is the speed of light.

The spectra taken from the ends of a nanowire 5.1 μm in length (SEM image in the inset) exhibited peaks with a periodic spacing characteristic of Fabry–Perot resonator modes (Figure 4B). The minima in the spectrum from the input end, and maxima in the spectrum of from the output end, correspond to the wavelengths at which maximum transmission occurred due to constructive interference of plasmons within the nanowire resonator.<sup>4</sup>

The spacing between the resonator modes is not constant because the phase velocity of the plasmons varies as a function of wavelength (Figure 4C). We calculated the phase

velocity as a function of wavelength with eq 1, using the wavelength difference between the peaks in the spectra from three nanowires of different lengths (4.4, 5.1, and 5.2  $\mu\text{m}$ ). The wavelength of the plasmon is approximately 283 nm at 1.75 eV and 491 nm at 1.38 eV. The wavelength of a plasmon is shorter than the wavelength of light in vacuum at the same frequency, and the rate of change of the wavelength per unit frequency is less than that of light in a vacuum. These results are similar to those obtained for silver nanowires.<sup>12</sup> The insets of Figure 4C illustrate the change in the plasmon wavelength of about 60% across this frequency range.

To compare the morphology and optical properties of single-crystalline nanowires produced by nanoskiving with those of polycrystalline nanowires, we fabricated polycrystalline nanowires by a three-step process: (i) patterning 5- $\mu\text{m}$ -wide gold lines on an epoxy substrate by electron-beam evaporation and a photolithographic lift-off process, (ii) embedding the patterned film in additional epoxy, and (iii) sectioning it with the ultramicrotome. The surface of the polycrystalline wire in Figure 4D appears much rougher than that of the single-crystalline nanowires. The polycrystalline wire also bent due to the inhomogeneous stress applied by the microtome blade. The remarkable smoothness and straightness of the single-crystalline wires indicates that the roughness and bending of polycrystalline wires is due to their polycrystallinity rather than the nanoskiving process itself and that nanoskiving produces nanostructures with the same smooth surfaces, straight edges, and single-crystalline structure as synthetic methods when performed on a synthetic (single-crystalline) starting material.

The spectrum from the input end of the polycrystalline wire has some small, broad periodic peaks, and the output spectrum displays no periodic peaks. These spectra indicate the polycrystalline plasmon resonator has greater loss than the single-crystalline wire. The relative greater loss is due to the scattering of surface plasmons from the rough surface of the polycrystalline wire; this emission is not allowed from a smooth surface due to the wavevector mismatch between the surface plasmons and light in air.<sup>13</sup>

The radiation of the surface plasmons from rough surfaces can be understood as polarization currents normal to the surface radiating as Hertzian dipoles.<sup>14</sup> A quantitative description of the emitted light  $dI$  per solid angle element  $d\Omega$  and per incident power  $I_0$  from a rough gold film is given by Kretschmann<sup>14</sup> as eq 2,

$$\frac{dI}{I_0 d\Omega} = \left(\frac{\pi}{\lambda}\right)^4 \frac{4\sqrt{\epsilon}}{\cos \theta_0} |t_p(\theta_0)|^2 |W|^2 |s_{k-k_0}|^2 \quad (2)$$

where  $\lambda$  is the wavelength of light in vacuum,  $\epsilon$  is the dielectric constant of the substrate (e.g., glass),  $\theta_0$  is the angle of incident light from normal,  $t_p$  describes the amplitude of the electric field at the metal–air interface,  $W$  describes the angular intensity of radiated light, and  $s_{k-k_0}$  is the Fourier transform of the roughness function. Equation 2 indicates that radiative loss should be greater at shorter wavelengths, and this relationship can be observed qualitatively in the spectra of Figure 4D.

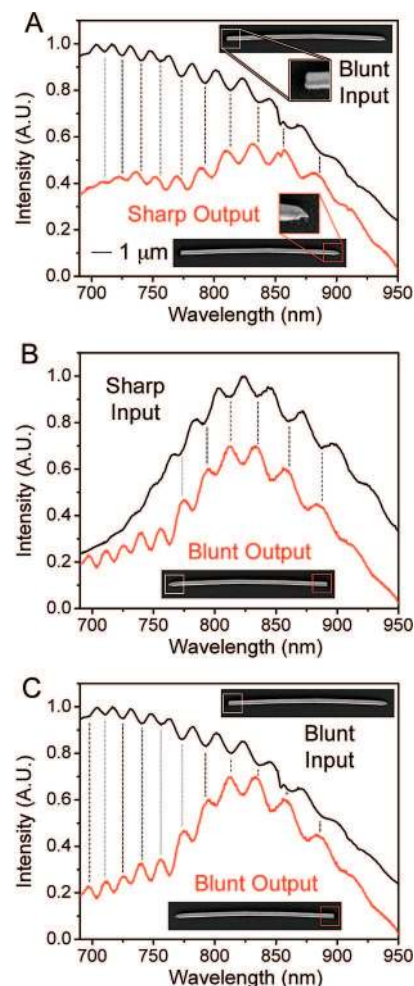


**Figure 5.** (A) Spectra from a nanowire with a blunt input and sharp output. The lack of correspondence between the minima of the reflection spectra (input) and the maxima of the transmission spectra (output) was caused by the asymmetry of the resonator. (B) Spectra from the same nanowire rotated by 180° shows that the sharp tip acted as an optical antennae, with a longitudinal resonance frequency of  $\sim 825$  nm. (C) The correspondence between the minima from the blunt input and the maxima from the blunt output confirm that the sharp tip caused the mismatch in (A).

The sharp tips at the ends of some nanowires present an opportunity to study how these tips affect the optical properties of the nanowires. Figure 5 shows spectra from a nanowire 8  $\mu\text{m}$  in length with one blunt end and one sharp end. If the blunt end served as the input (Figure 5A), the spectra from the blunt end and sharp end both exhibited peaks with a periodic frequency spacing, but the minima of the input were offset from the maxima of the output, with a greater offset at shorter wavelengths. The asymmetry of this nanowire resonator caused a mismatch between the maxima of the transmittance and minima of the reflectance spectra.

If the wire was rotated 180°, such that the sharp end served as the input, the scattering spectra exhibited a broad peak centered at 825 nm, with a superimposed Fabry–Perot interference pattern. This result suggests that the sharp tip acted as a local plasmon resonator, or optical antennae, strongly scattering light at a frequency red-shifted from the surface plasmon resonance frequency of bulk gold films ( $\sim 610$  nm).<sup>15</sup> Gold nanorods with an aspect ratio of  $\sim 4.5$

strongly scatter light at a similar frequency as the tip of this nanowire due to longitudinal plasmon resonance.<sup>16</sup> The increase in scattered light from the blunt *output* at 825 nm suggests that the localized plasmon resonance of the sharp, nanoscale antennae increased the coupling of light into the propagating plasmon mode along the nanowire.

To confirm that the sharp tip caused the mismatch between the transmittance and reflectance spectra, we plotted the spectra from the blunt input with the spectra from the blunt output (Figure 5C). The spectra exhibited the expected correspondence between the minima of the input and maxima of the output.

**Conclusion.** Nanoskiving of chemically synthesized, single-crystalline microplates of gold produces collinearly aligned, single-crystalline nanowires with very smooth surfaces (much smoother than those obtained by nanoskiving polycrystalline thin films). Successive sections from microplates produce nanowires with smoothly modulated dimensions. Correlation of the optical properties of nanowires in each section (<1 mm<sup>2</sup>) with SEM images of their structure is greatly simplified by the low number of nanowires in each section, their collinear alignment, and their random but reproducible spacing. The smooth surfaces of the gold nanowires produced by this process allow them to serve as surface plasmon resonators.

Nanoskiving of chemically synthesized, single-crystalline materials makes possible the fabrication and study of new structures for nanophotonics and nanomaterials research. For example, in addition to preparation of collinear nanowires, one might also deposit a thin dielectric layer between two layers of microplates to make plasmonic slot waveguides. Nanoskiving of other two-dimensional (silver and palladium nanoplates) and one-dimensional nanostructures (metal and semiconductor nanowires) will, we believe, bring a new level of control to their dimensions and relative positions and help elucidate the effect of size and shape on their optical and electronic properties.

**Acknowledgment.** We acknowledge support from the Defense Advanced Research Projects Agency (DARPA) under award no. HR0011-04-1-0032 and The California Institute of Technology. F.C. acknowledges support from the Air Force Office of Scientific Research (AFOSR) MURI on Plasmonics, and G.M.W. and F.C. both acknowledge support from the Harvard Nanoscale Science and Engineering Center (NSEC). This work was performed in part at the Center for Nanoscale Systems (CNS), a member of the National Nanotechnology Infrastructure Network (NNIN), which is supported by the National Science Foundation under NSF award no. ECS-0335765. CNS is part of the Faculty of Arts and Sciences at Harvard University.

**Supporting Information Available:** Experimental section. This material is available free of charge via the Internet at <http://pubs.acs.org>.

## References

- (1) Ditlbacher, H.; Hohenau, A.; Wagner, D.; Kreibitz, U.; Rogers, M.; Hofer, F.; Aussenegg, F.; Krenn, J. *Phys. Rev. Lett.* **2005**, *95*, 257403.
- (2) Barnes, W. L.; Dereux, A.; Ebbesen, T. W. *Nature* **2003**, *424*, 824.
- (3) Yatsui, T.; Kourogi, M.; Ohtsu, M. *Appl. Phys. Lett.* **2001**, *79*, 4583.
- (4) Krenn, J. R.; Lamprecht, B.; Ditlbacher, H.; Schider, G.; Salerno, M.; Leitner, A.; Aussenegg, F. R. *Europhys. Lett.* **2002**, *60*, 663.
- (5) Elechiguerra, J. L.; Larios-Lopez, L.; Liu, C.; Garcia-Gutierrez, D.; Camacho-Bragado, A.; Yacaman, M. J. *Chem. Mater.* **2005**, *17*, 6042.
- (6) Xu, Q.; Rioux, R. M.; Whitesides, G. M. *ACS Nano* **2007**, *1*, 215.
- (7) Xu, Q.; Bao, J.; Capasso, F.; Whitesides, G. *Angew. Chem., Int. Ed.* **2006**, *45*, 3631.
- (8) Xu, Q.; Bao, J.; Rioux, R. M.; Perez-Castillejos, R.; Capasso, F.; Whitesides, G. M. *Nano Lett.* **2007**, *7*, 2800.
- (9) Xu, Q.; Gates, B. D.; Whitesides, G. M. *J. Am. Chem. Soc.* **2004**, *126*, 1332.
- (10) Xu, Q.; Perez-Castillejos, R.; Li, Z.; Whitesides, G. M. *Nano Lett.* **2006**, *6*, 2163.
- (11) Kan, C.; Zhu, X.; Wang, G. *J. Phys. Chem. B* **2006**, *110*, 4651.
- (12) Allione, M.; Temnov, V. V.; Fedutik, Y.; Woggon, U.; Artemyev, M. V. *Nano Lett.* **2008**, *8*, 31.
- (13) Raether, H., *Surface Plasmons on Smooth and Rough Surfaces and on Gratings*; Springer-Verlag: Berlin, 1988.
- (14) Kretschmann, E. *Opt. Commun.* **1972**, *5*, 331.
- (15) Kapitza, H. *Opt. Commun.* **1976**, *16*, 73.
- (16) Huang, X.; El-Sayed, I. H.; Qian, W.; El-Sayed, M. A. *J. Am. Chem. Soc.* **2006**, *128*, 2115.

NL802252R